JOC Article

Time-Resolved Resonance Raman and Density Functional Theory Study of the Deprotonation Reaction of the Triplet State of *p*-Hydroxyacetophenone in Water Solution

Peng Zuo, Chensheng Ma, Wai Ming Kwok, Wing Sum Chan, and David Lee Phillips*

Department of Chemistry, The University of Hong Kong, Pokfulam Road, Hong Kong S.A.R., P.R. China

phillips@hku.hk

Received April 15, 2005

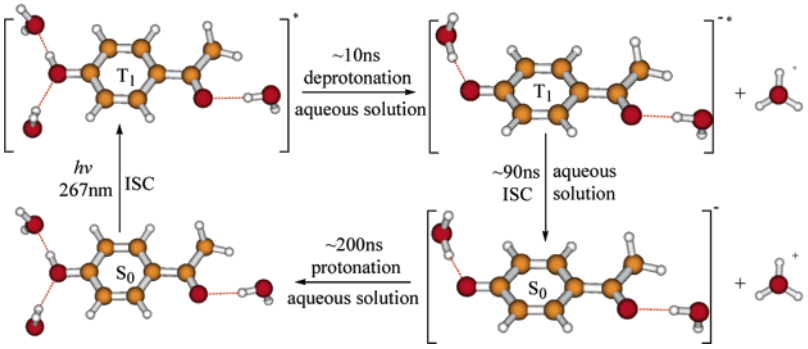

Picosecond and nanosecond time-resolved resonance Raman (TR^3) spectroscopy was employed to investigate the deprotonation/ionization reaction of *p*-hydroxyacetophenone (HA) after ultraviolet photolysis in water solution. The TR^3 spectra in conjunction with density functional theory (DFT) calculations were used to characterize the structure and dynamics of the excited-state HA deprotonation to form HA anions in near neutral water solvent. DFT calculations based on a solute−solvent intermolecular H-bonded complex model containing up to three water molecules were used to evaluate the H-bond interactions and their influence on the deprotonation reaction and the structures of the intermediates. The deprotonation reaction was found to occur on the triplet manifold with a planar H-bonded HA triplet complex as the precursor species. The HA triplet species is generated within several picoseconds and then decays with a ~10 ns time constant to produce the HA triplet anion species after 267 nm photolysis of HA in water solution. The triplet anion species was observed to decay with a time constant of about 90 ns into the ground-state anion species that was found to have a lifetime of about 200 ns. The DFT calculations on the H-bonded complexes of the anion triplet and ground-states species suggest that these anion species are H-bonded complexes with planar quinonoidal structures containing two water molecules H-bonded, respectively, with oxygen lone pairs of the carbonyl and deprotonated hydroxyl moieties. A deactivation scheme of the photoexcited HA in regard to the deprotonation reaction in neutral water solutions was proposed. With the above dynamic and structural information available, we briefly discuss the possible implications of the model HA photochemistry in water solutions for the photodeprotection reactions of related *p*-HP phototrigger compounds in aqueous solutions.

Introduction

Compounds with photochemically removable protecting groups are sometimes named "caged molecules" or "phototriggers" when they are employed for biochemical applications,[1−4] and these types of compounds are also important in multistep synthesis, combinatorial chemistry, and photolithographic technology.[1−13] A number of protecting groups have been reported, and much interest has recently focused on the aromatic α-keto class of molecules since some of them may have potential use as

* Author to whom correspondence should be addressed. Fax: 852-2857-1586.

(1) (a) Givens, R. S.; Kueper, L. W. *Chem. Rev.* **1993**, *93*, 55−66 and references therein. (b) Givens, R. S.; Athey, P. S.; Matuszewski, B.; Kueper, L. W., III; Xue, J. Y.; Fister, T. *J. Am. Chem. Soc.* **1993**, *115*, 6001−6012 and references therein. (c) Gee, K. R.; Kueper, L. W., III; Barnes, J.; Dudley, G.; Givens, R. S. *J. Org. Chem.* **1996**, *61*, 1228−1233.

10.1021/jo050761q CCC: $30.25
Published on Web 09/24/2005

efficient phototriggers for the release of a variety of biological stimulants.[1−6] Particular interest has been paid to the *p*-hydroxyphenacyl (*p*-HP) type of aromatic α-keto class of molecules because they appear to undergo the desired photorelease reaction (liberation of the protected group and a *p*-hydroxyphenacylacetic rearrangement product) exclusively in water or solvents with appreciable amounts of water present.[3,4a,6,8] It is important to understand the role of water in aqueous solutions to better understand the deprotection reaction mechanism in these types of compounds. This area has been examined in several studies using techniques such as time-resolved transient absorption spectroscopy and product analysis,[1,3,4a,6] and much has been learned about these reactions, but there still remains a number of unresolved issues and some conflicting interpretations about the deprotection mechanism(s) in these types of aromatic α-keto compounds.

We have recently begun to use time-resolved resonance Raman spectroscopy (TR^3) to directly probe the structure and properties of intermediates involved in selected *p*-HP photorelease compounds.[14,15] TR^3 in conjunction with femtosecond Kerr gated time-resolved fluorescence (KTRF) were used to examine the early time photophysics of *p*-hydroxyacetophenone (HA) and several *p*-HP phototriggers in neat acetonitrile (MeCN) and in 50% H_2O/50% CH_3CN (v/v) mixed solution,[14,15] and these studies showed that intersystem crossing (ISC) is very fast with the triplet formation taking place with a rate of about 5×10^{11} s^{-1} in both solvent systems. These experiments also showed that the triplet state lifetime is very leaving group dependent with the lifetimes becoming substantially shorter in the water-mixed solvent compared to that of a neat MeCN solvent. This indicates the triplet state is most probably the reactive precursor for the *p*-HP deprotection reaction[14] as has been assigned by Givens, Wirz, and co-workers.[3,4a] It is important to understand the structure, properties, and chemical reactions of both the HA model compound and its *p*-HP phototriggers with and without water present to better understand their aqueous phase reactions.

Previous mechanistic studies indicate that a series of fast steps are involved in the *p*-HP photorelease reaction.[3,4a,6] Among these, the deprotonation of the *p*-HP hydroxy moiety, a process that can occur only in water-containing solvents, has been proposed to be one of the most important events to facilitate the release of the leaving group.[3,6] Although this appears to be reasonable, solid and unequivocal experimental evidence to validate such a viewpoint, such as the identification and dynamics of the associated intermediate(s), is absent to the best of our knowledge. Understanding the photochemistry and related dynamics of the HA model compound provides an indication of the intrinsic property of the deprotonation reaction for the *p*-HP chromophore. Availability of this information is essential to evaluate the role of the deprotonation process in the *p*-HP deprotection process.

Fast photoinduced deprotonation of HA in water solution has been noted by an early laser flash photolysis (LFP) study by Porter and co-workers and was associated with the increased acidity of the hydroxy moiety in the excited state in relation to the ground state.[16] Recently, by using transient absorption (TA) spectroscopy, Wirz and co-workers reinvestigated the prototropic equilibrium of the excited-state HA in largely water-mixed acetonitrile solution.[4a] Several short-lived species have been observed under neutral condition and buffered solvents with various pH values. Although tentative assignments of the intermediates were proposed, additional work, especially studies using vibrational spectroscopy, is needed to corroborate the assignment as well as to provide information about the structures of and the dynamics of conversion among these species. In this regard, we report in this paper a time-resolved resonance Raman (TR^3) study of the deprotonation reaction of the HA model compound in water solution. By comparison with our previous TR^3 work on HA in neat acetonitrile,[15b] our present work reveals that the HA excited-state deprotonation occurs on the triplet manifold leading to generation of the triplet anion that further deactivates by intersystem crossing (ISC) to the ground-state anion. Unambiguous identification of the anion triplet and ground-state species were corroborated by our TR^3 results on selected isotopically labeled compounds and were additionally confirmed by density functional theory (DFT) calculations. We also obtained time constants for the dynamics of formation of these anion intermediates.

Our recent work on *p*-methoxyacetophenone (MAP) reveals that, in water and largely water-containing solvent, the intermolecular H-bond between MAP and the solvent water molecule can lead to significant modification of the nature of the triplet state compared to that of

(2) Givens, R. S.; Athey, P. S.; Kueper, L. W., III; Matuszewski, B.; Xue, J.-Y. *J. Am. Chem. Soc.* **1992**, *114*, 8708−8710.
(3) (a) Gives, R. S.; Park, C.-H. *Tetrahedron Lett.* **1996**, *37*, 6259−6262. (b) Park, C.-H.; Givens, R. S. *J. Am. Chem. Soc.* **1997**, *119*, 2453−2463. (c) Givens, R. S.; Jung, A.; Park, C.-H.; Weber, J.; Bartlett, W. *J. Am. Chem. Soc.* **1997**, *119*, 8369−8370. (d) Givens, R. S.; Weber, J. F. W.; Conrad, P. G., II; Orosz, G.; Donahue, S. L.; Thayer, S. A. *J. Am. Chem. Soc.* **2000**, *122*, 2687−2697 and references therein. (e) Conrad, P. G., II; Givens, R. S.; Weber, J. F. W.; Kandler, K. *Org. Lett.* **2000**, *2*, 1545−1547.
(4) (a) Conrad, P. G., II; Givens, R. S.; Hellrung, B.; Rajesh, C. S.; Ramseier, M.; Wirz, J. *J. Am. Chem. Soc.* **2000**, *122*, 9346−9347. (b) Il'ichev, Y. V.; Schworer, M. A.; Wirz, J. *J. Am. Chem. Soc*. **2004**, *126*, 4581−4595. (c) Rajesh, C. S.; Givens, R. S.; Wirz, J. *J. Am. Chem. Soc.* **2000**, *122*, 611−618. (d) Hangarter, M.-A.; Hörmann, A.; Kamdzhilov, Y.; Wirz, J. *Photochem. Photobiol. Sci.* **2003**, *2*, 524−535.
(5) (a) Banerjee, A.; Falvey, D. E. *J. Am. Chem. Soc.* **1998**, *120*, 2965−2966. (b) Lee, K.; Falvey, D. E. *J. Am. Chem. Soc.* **2000**, *122*, 9361−9366. (c) Banerjee, A.; Lee, K.; Yu, Q.; Fan, A. G.; Falvey, D. E. *Tetrahedron Lett.* **1998**, *39*, 4635−4638. (d) Banerjee, A.; Falvey, D. E. *J. Org. Chem.* **1997**, *62*, 6245−6251.
(6) (a) Zhang, K.; Corrie, J. E. T.; Munasinghe, V. R. N.; Wan, P. *J. Am. Chem. Soc.* **1999**, *121*, 5625−5632. (b) Brousmiche, D. W.; Wan, P. *J. Photochem. Photobiol., A* **2000**, *130*, 113−118.
(7) Namiki, S.; Arai, T.; Fujimori, K. *J. Am. Chem. Soc.* **1997**, *119*, 3840−3841.
(8) Sheehan, J. C.; Umezawa, K. *J. Org. Chem.* **1973**, *38*, 3771−3774.
(9) Pelliccioli, A. P.; Wirz, J. *Photochem. Phobiol. Sci.* **2002**, *1*, 441−458.
(10) Falvey, D. E.; Sundarajan, C. *Photochem. Phobiol. Sci.* **2004**, *3*, 831−838.
(11) Bochet, C. G. *J. Chem. Soc., Perkin Trans. 1* **2002**, *2*, 125−142.
(12) Pillai, V. N. R. *Synthesis*, **1980**, 1−26.
(13) Zabadal, M.; Klan, P. *Chem. Listy* **2001**, *95*, 694−699.
(14) Ma, C.; Kwok, W. M.; Chan, W. S.; Zuo, P.; Kan, J. T. W.; Toy, P. H.; Phillips, D. L. *J. Am. Chem., Soc.* **2005**, *127*, 1463−1472.
(15) (a) Ma, C.; Chan, W. S.; Kwok, W. M.; Zuo, P.; Phillips, D. L. *J. Phys. Chem. B* **2004**, *108*, 9264−9276. (b) Ma, C.; Zuo, P.; Kwok, W. M.; Chan, W. S.; Kan, J. T. W.; Toy, P. H.; Phillips, D. L. *J. Org. Chem.* **2004**, *69*, 6641−6657.
(16) (a) Porter, G.; Suppan, P. *Trans. Faraday Soc.* **1965**, *61*, 1664−1673. (b) Beckett, A.; Porter, G. *Trans. Faraday Soc.* **1963**, *59*, 2051−2057.

the free MAP triplet state.[17] Given the closely related structures between MAP and HA, a similar H-bond effect is expected to apply also to the HA triplet and could consequently influence the triplet deprotonation reaction. A similar H-bond effect was found here in the DFT calculations on a series of H-bonded complexes of HA containing up to three water molecules. These results are discussed in terms of the structural change upon going from the neutral to the anion HA triplet associated with the triplet deprotontaiton reaction. To our knowledge, this represents the first time-resolved vibrational spectroscopic observation of the HA deprotonation process and characterization of the anion products. We discuss briefly the photochemistry of the HA model compound in water solutions and possible implications for the photorelease reaction of related *p*-HP phototrigger compounds.

Experimental and Computational Methods

Natural abundance *p*-hydroxyacetophenone (HA) is available commercially and was used after recrystallization. HA-^{13}C and HA-D_4 isotopically labeled compounds (shown below) were synthesized and characterized as previously described in ref 15b. Spectroscopic grade acetonitrile and deionized water were used as solvents to prepare samples for the TR^3 experiments. The following buffer was used in the water samples: pH 9.0 (acetate + phosphate + borate, I = 0.1 M).

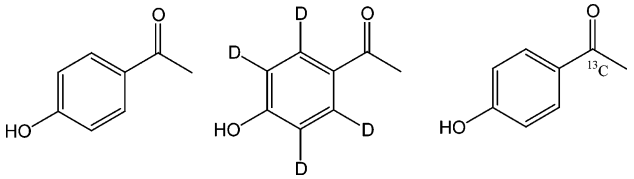

HA HA-D_4 HA-^{13}C

The ps-TR^3 experiments were done using a recently developed ultrafast laser system in this laboratory that has been described elsewhere,[14,15] and only a very brief description will be provided here. The Ti:Sapphire regenerative amplifier laser system was operated in the picosecond mode and had a 800 nm, ~1 ps, and 1 kHz output. Samples in the ps-TR^3 experiments were pumped with a 267 nm wavelength and probed with a 400 nm wavelength. The 267 nm pump and 400 nm probe wavelengths were generated from the third and second harmonics of the 800 nm output from the regenerative amplifier, respectively. The pulse energies incident on the sample were about 2−3 μJ and the time resolution of the system was ~2 ps. The Raman scattered light was collected using a backscattering geometry and passed through a 0.5 spectrograph whose grating dispersed the light onto a liquid nitrogen cooled CCD detector.

The ns-TR^3 measurements were done using an apparatus described previously in ref 18. A 266 nm pump and 416 and 341.5 nm probe excitation wavelengths were used in the experiments and generated from the harmonics of a 10 Hz pulsed Nd:YAG laser and/or their hydrogen Raman-shifted laser lines. The time delay between the pump and probe beams was controlled electronically using a pulse generator, and the time resolution of the experiments is ~10 ns. The excitation geometry and the light collection geometry were similar to those used in the picosecond experiments. A sample concentration of ~1 mM is used for both the ps- and ns-TR^3 measurements.

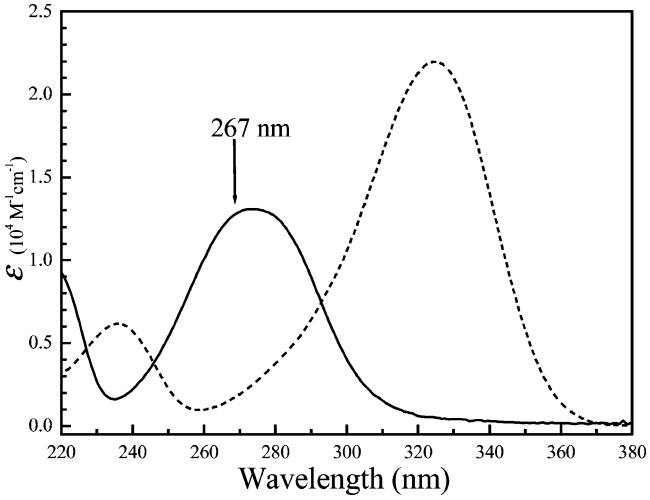

FIGURE 1. UV absorption spectra of HA in water (solid line, λ_{max} = 274.5 nm, ϵ = 13 000 M^{-1} cm^{-1}) and in water/NaOH (0.1 M) (dashed line, λ_{max} = 325 nm, ϵ = 22 000 M^{-1} cm^{-1}) solution.

The optimized geometry, frequency, and Raman activity of vibrational mode were calculated from B3LYP/6-311G(d,p) density functional theory (DFT) computations for the ground-state species of HA and from open-shell UB3LYP functionals for the triplet state species examined here. Analogous calculations were also done for the corresponding H-bonded complexes with one, two, and three water molecules being H-bonded with the hydroxy hydrogen and lone pairs of the carbonyl oxygen and hydroxy oxygen, respectively. For all the H-bonded complexes, the H-bond stabilization energy required for the complexes dissociating into free HA and water molecules were estimated based on the total energy (including zero-point energy, ZPE) calculated for the corresponding species. Vibrational analysis confirmed all of the stationary points obtained were minima. Frequency calculations were also done for triplet states of HA-^{13}C and HA-D_4 to theoretically predict the isotope effect and to compare to experimental data. All of the calculations were done employing the Gaussian 98 program suite.[19]

Results and Discussion

A. TR^3 Observation of the Triplet Deprotonation Reaction of HA in Water Solutions. Figure 1 shows the absorption spectrum of HA in neutral water and 0.1 M NaOH/water solutions. The spectrum in neutral water is from neutral HA, while the one in NaOH solution is

(17) Chan, W. S.; Ma, C.; Kwok, W. M.; Phillips, D. L. *J. Phys. Chem. A* **2005**, *109*, 3454−3469.

(18) (a) Li, Y.-L.; Leung, K. H.; Phillips, D. L. *J. Phys. Chem. A* **2001**, *105*, 10621−10625. (b) Li, Y.-L.; Chen, D. M.; Wang, D.; Phillips, D. L. *J. Org. Chem.* **2002**, *67*, 4228−4235. (c) Li, Y.-L.; Wang, D.; Phillips, D. L. *J. Chem. Phys.* **2002**, *117*, 7931−7941. (d) Ong, S. Y.; Zhu, P.; Poon, Y. F.; Leung, K.-H.; Fang, W. H. *Chem. Eur. J.* **2002**, *8*, 2163−2171. (e) Ong, S. Y.; Chan, P. Y.; Zhu, P.; Leung, K. H.; Phillips, D. L. *J. Phys. Chem. A* **2003**, *107*, 3858−3865. (f) Chan, P. Y.; Kwok, W. M.; Lam, S. K.; Chiu, P.; Phillips, D. L. *J. Am. Chem. Soc.* **2005**, *127*, 8246−8247.

(19) Frisch, M. J.; Trucks, G. W.; Schlegel, H. B.; Scuseria, G. E.; Robb, M. A.; Cheeseman, J. R.; Zakrzewski, V. G.; Montgomery, J. A., Jr.; Stratmann, R. E.; Burant, J. C.; Dapprich, S.; Millam, J. M.; Daniels, A. D.; Kudin, K. N.; Strain, M. C.; Farkas, O.; Tomasi, J.; Barone, V.; Cossi, M.; Cammi, R.; Mennucci, B.; Pomelli, C.; Adamo, C.; Clifford, S.; Ochterski, J.; Petersson, G. A.; Ayala, P. Y.; Cui, Q.; Morokuma, K.; Malick, D. K.; Rabuck, A. D.; Raghavachari, K.; Foresman, J. B.; Cioslowski, J.; Ortiz, J. V.; Baboul, A. G.; Stefanov, B. B.; Liu, G.; Liashenko, A.; Piskorz, P.; Komaromi, I.; Gomperts, R.; Martin, R. L.; Fox, D. J.; Keith, T.; Al-Laham, M. A.; Peng, C. Y.; Nanayakkara, A.; Gonzalez, C.; Challacombe, M.; Gill, P. M. W.; Johnson, B.; Chen, W.; Wong, M. W.; Andres, J. L.; Gonzalez, C.; Head-Gordon, M.; Replogle, E. S.; Pople, J. A. *Gaussian 98*, revision A.7; Gaussian, Inc.: Pittsburgh, PA, 1998.

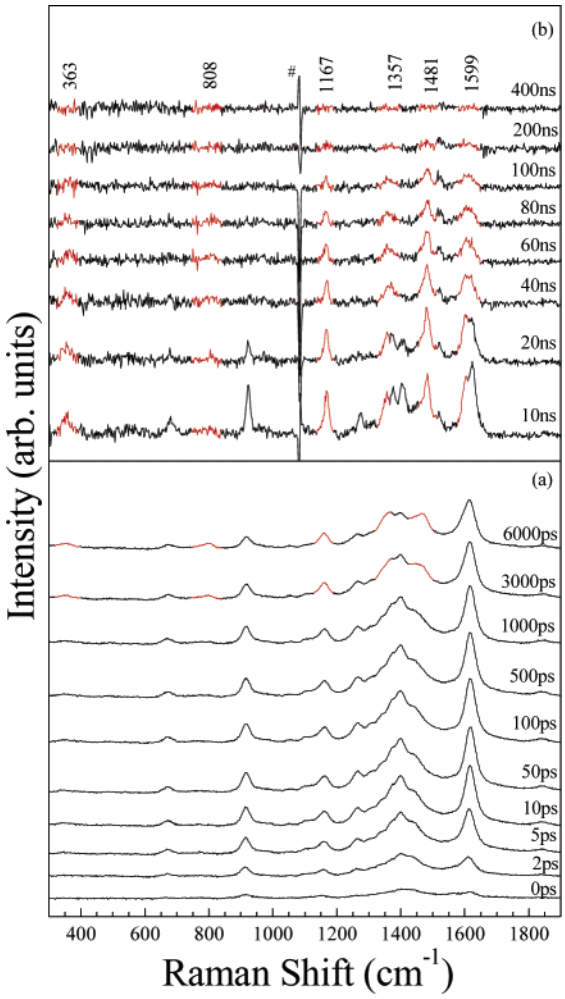

FIGURE 2. Picosecond-TR^3 (a) and nanosecond-TR^3 (b) spectra of HA in water solution obtained at various time delays with 267 nm pump and 400 nm probe wavelengths for the picosecond spectra and 266 nm pump and 416 nm probe wavelengths for the nanosecond spectra. The band labeled by the # is due to a stray laser line.

from the ionized HA anion ground-state species. The 267 nm pump wavelength used in the TR^3 measurements is indicated by an arrow in the figure.

Figure 2 displays representative ps- and ns-TR^3 spectra of HA obtained in water solvent, and Figure 1S in the Supporting Information provides an overview of all the spectra obtained in this solvent. The ps-TR^3 spectra were acquired using 267 nm pump and 400 nm probe excitation wavelengths, while the ns-TR^3 spectra were obtained using 266 nm pump and 416 nm probe wavelengths. The Raman bands in the ps-TR^3 spectra are broad due to the convolution of the intrinsic Raman bandwidth with the relatively large line width of the picosecond laser pulses ($\sim$15 cm^{-1}). The ns-TR^3 spectra have better resolution due to the narrower line width of the nanosecond laser ($\sim$1 cm^{-1}), and this allows spectral features to be better resolved in the ns-TR^3 spectra than in the ps-TR^3 spectra.

Inspection of Figure 2 reveals that the TR^3 measurement with the 400 or 416 nm probe wavelengths leads to detection of two different transient species in water solvent. This is different from the corresponding TR^3 result we reported for HA in acetonitrile[15b] where only one transient assigned to the triplet state of HA was observed. Our recent time-resolved fluorescence study shows that, for HA and *p*-HP phototrigger compounds, the ISC is rapid with a time constant of $\sim$2 ps and the conversion rates in water and water-mixed acetonitrile are rather similar to those observed in neat acetonitrile.[14] According to this, it is straightforward that the first species observed in Figure 2 (0−1000 ps spectra) is due to the HA triplet. However, comparison of the triplet spectra reported here in water solution with those of the previous result in acetonitrile solvent[15b] reveals some obvious differences in the frequencies of many of the vibrational features as well as spectral profile. These differences parallel the triplet TR^3 result we obtained for the closely related compound MAP in the water-mixed acetonitrile vs neat acetonitrile,[17] and this can be associated with the triplet state solute−solvent intermolecular H-bond effect. As illustrated below in section D, this is indeed confirmed by the DFT-calculated results for comparison of the free HA triplet and the HA−water H-bonded triplet complexes. To differentiate the H-bonded triplet from the normal free HA triplet (designated as ^{3}HA hereafter), we signify the H-bonded HA triplet as ^{3}HA′. It is known that, like that of the MAP ground-state species,[17] the ground-state HA molecule is H-bonded with the surrounding water molecules at both the hydroxy and carbonyl sites in water solution (the free and H-bonded ground-state HA is designated as HA and HA′, respectively). The H-bonding interaction between the carbonyl moiety and the solvent water molecule(s) is manifested clearly by the much broader C=O stretching Raman bandwidth recorded in water compared to that in acetonitrile solvent (the Raman spectra are displayed in Figure 2S in the Supporting Information). The early picosecond spectra in Figure 2 show rapid growth of the H-bonded ^{3}HA′ triplet species. Analogous to the case of MAP,[17] it is reasonable that the ^{3}HA′ triplet state stems from the modified form of the corresponding H-bonded HA′ ground state. This is corroborated with the DFT results (below) showing that the H-bond conformations for the triplet complexes are not very different from their ground-state counterparts, while strengths of the H-bonds are stronger in the triplet than the ground-state complex.

Our previous TR^3 study on HA shows that the free ^{3}HA triplet has a lifetime of $\sim$40 ns in acetonitrile.[15b] The reader is referred to ref 15b for details of the vibrational assignments of the ^{3}HA TR^3 spectra. However, as displayed in Figure 2, the ^{3}HA′ species decays within 10 ns in water and transfers directly into another species as shown by the appearance of new Raman bands at, for example, 1167, 1357, 1481, and 1599 cm^{-1} (the features in red as displayed in Figure 2). The time constant for conversion of the ^{3}HA′ triplet to the new species can be estimated to be roughly $\sim$10 ns due to limitations in the time resolution of the present TR^3 measurement. Decay of this new transient species follows a one-exponential function with a time constant of 95 ns under open-air conditions. The decay kinetics together with the exponential fitting is displayed in Figure 3. To test the effect of oxygen on the decay, the ns-TR^3 measurements were also done with purging of the sample solution with nitrogen. The decay of the new species was found to be noticeably slower with a N_2 purge, and a $\sim$140 ns decay

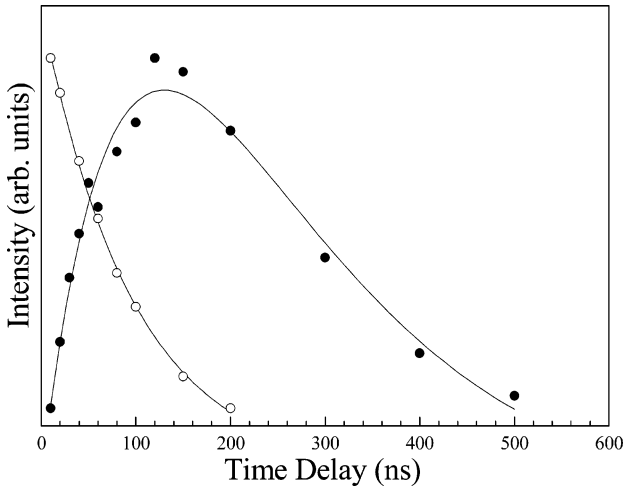

FIGURE 3. Kinetics of the HA triplet anion (hollow circles) and the ground-state anion (solid circles) observed in the ns-TR^3 spectra of HA in neutral water solution. The time dependence of the anion triplet state is obtained by using the temporal change of the 1481 cm^{-1} band area in the ns-TR^3 spectra displayed in Figure 2b; the time dependence of the anion ground state was obtained from the temporal change of the 705 cm^{-1} band area in the ns-TR^3 spectra displayed in Figure 7.

time constant was found (see the decay of the transient signal under N_2 purge condition given in Figure 3S in the Supporting Information). This suggests the new species is probably triplet in nature.

We performed similar TR^3 experiments in a basic water solution (pH = 9.0 buffer), and the spectra obtained are shown in Figure 4. The ns-TR^3 spectra (Figure 4b) exhibit only the new triplet species. Comparison with the corresponding result in neutral water solvent (Figure 2b) reveals that the new triplet species is formed faster in basic solution than under neutral conditions. This is substantiated by the ps-TR^3 spectra displayed in Figure 4a. Although the S/N ratio of the spectra is moderate and there is strong overlap between the features of the ^{3}HA′ and those of the new species, it is quite certain that the conversion time constant under basic conditions is faster than that in neutral water solvent. Since one may expect that deprotonation of the ^{3}HA′ species could be faster in basic solution compared to that in a near neutral solution, we tentatively assign the new triplet species to the triplet anion of HA formed from the ^{3}HA′ deprotonation (or ionization) reaction. This assignment is consistent with previous nanosecond LFP studies done by Givens, Wirz, and co-workers[4a] that observed that the TA spectra of HA triplet and HA triplet anion are very similar. The direct excitation of the ground-state anion to form the anion triplet can be excluded since the ground-state anion shows very little absorption at the pump (267 nm) and probe (400 or 416 nm) wavelengths used in the TR^3 experiments (see the ultraviolet absorption spectrum of HA in NaOH/water solution displayed in Figure 1).

The solvent isotopic effect is known to be particularly informative in examining the proton transfer related dynamics and is thus expected to be important in support of the triplet anion assignment. Unfortunately, the expected isotopic effect dynamics could not be detected explicitly by the present TR^3 measurements because the

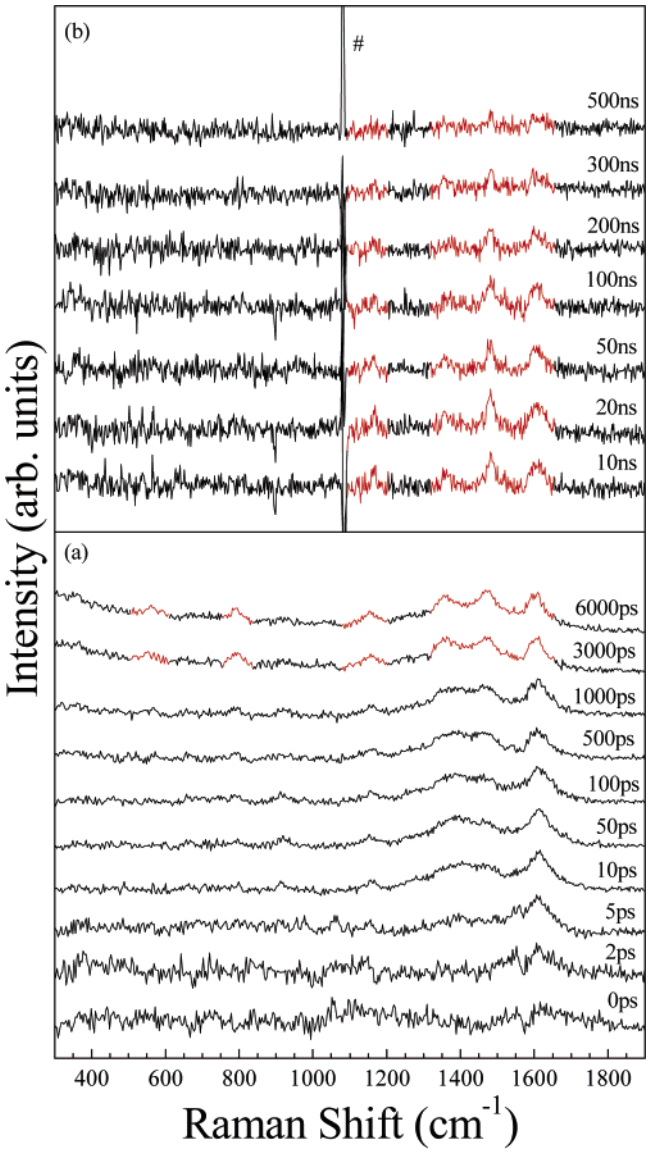

FIGURE 4. Picosecond-TR^3 (a) and nanosecond-TR^3 (b) spectra of HA in buffered water solution with pH = 9.0 obtained at various time delays with 267 nm pump and 400 nm probe excitation wavelengths for the picosecond spectra and 266 nm pump and 416 nm probe wavelengths for the nanosecond spectra. The band labeled by the # is due to a stray laser line.

roughly ~10 ns deprotonation time is beyond the 0−6000 ps detection time window of the ps-TR^3 measurement and within the ~10 ns time resolution of the ns-TR^3 measurement. To further corroborate the triplet anion assignment, a control experiment has been performed intending to obtain the 416 nm probed triplet anion spectrum by directly pumping the conjugate base with a 320 nm excitation wavelength (the maximum of the base, see Figure 1) in 0.1 M NaOH/water solution. Unfortunately, the attempt proved to be unsuccessful, and that is likely an indication of an inefficient ISC conversion of the excited conjugate base resulting in a low yield of the triplet anion species. This is confirmed by a transient absorption measurement performed in this lab that reveals a rapid recovery (with ~5 ps time constant, see Figure 4S in the Supporting Information) of the ground-

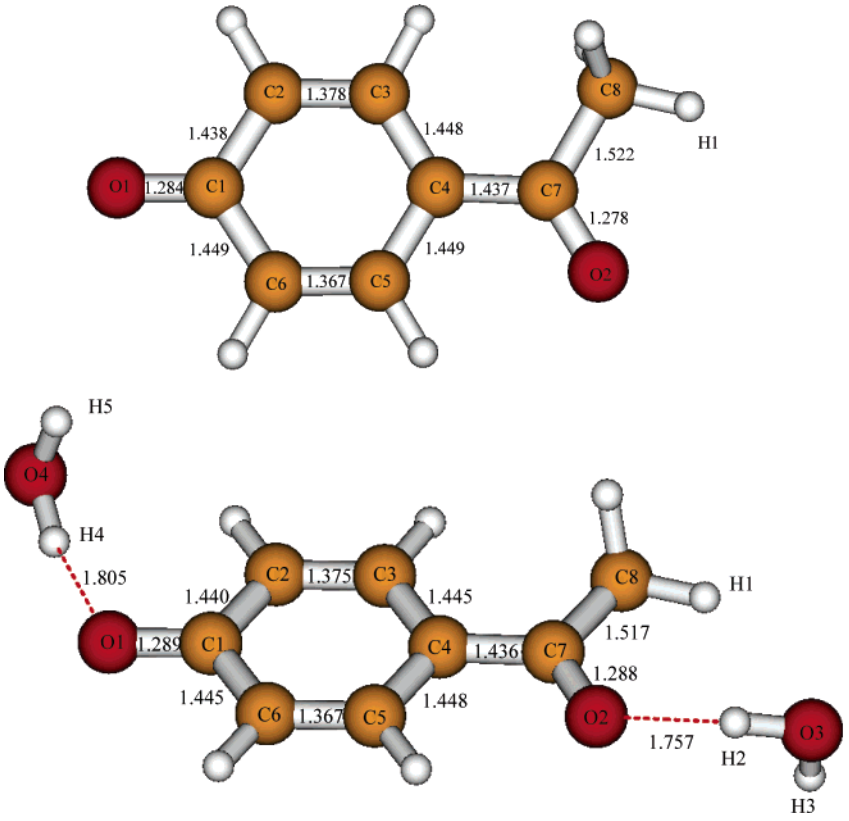

FIGURE 5. Optimized geometry of the free HA triplet anion and the anion triplet complex containing two water molecules H-bonded with the HA oxygen lone pairs of the carbonyl and deprotonated hydroxy moieties. The structure was obtained from DFT calculations using the UB3LYP method with a 6-311G(d,p) basis set. Bond lengths (in Å) are labeled for the C−C, C−O, and H-bond associated bonds.

state bleach for excitation of the HA conjugate base in the NaOH solution. This indicates that internal conversion (IC) to the ground state is likely the predominant deactivation pathway of the HA singlet excited state populated by photoexcitation. We note in this aspect, that the low yield of the HA triplet anion from the ground-state anion has been mentioned in previous work by Wirz and co-workers.[4a] It can be seen below that the triplet anion assignment has been firmly confirmed by the comparison of the experimental data with the DFT-calculated results.

B. Assignment of the HA Triplet Anion TR³ Spectrum. Temporal evolution of the TR³ spectra discussed above shows that the HA triplet anion originates from the H-bonded triplet complex ^{3}HA′. It is thus reasonable that the triplet anion is also in the form of an H-bonded complex. To determine the structure of the triplet anion and explore the influence of H-bonding interaction on the structure, UB3LYP/6-311G(d,p) DFT calculations were done to find the optimized geometry, vibrational frequencies, and predicted Raman spectrum for free HA triplet anion (denoted as ^{3}HA$^-$ hereafter) and anion triplet complexes (^{3}HA′$^-$) with the water molecule(s) H-bonded to the oxygen lone pairs of the carbonyl and deprotonated hydroxy groups. Figure 5 presents a simple schematic of the computed optimized geometry of the free HA triplet anion and the anion triplet H-bonded with two water molecules (denoted as ^{3}HA′−2H$_2$O) with the atoms numbered. The optimized structures of the anion triplet complex H-bonded with one water molecule at the carbonyl and hydroxy oxygen, respectively, are displayed in Figure 5S in the Supporting Information. Table 1S in the Supporting Information presents selected structural parameters for the ^{3}HA$^-$ and ^{3}HA′$^-$−2H$_2$O. Corresponding structural data for the anion triplet complex with one H-bonded water molecule are listed in Table 2S in the Supporting Information. The calculated total energies and stabilization energies for the H-bonded complexes are given in the respective tables. The triplet anion has a planar conformation with the structural modification caused by the H-bonds being quite local in nature. For example, the H-bonds lead to only a slight increase in the bond lengths (by less than 0.01 Å) for the C1−O1 and C7−O2 bonds that are directly associated with the H-bond interactions accompanied by little change to the other major geometric parameters. The calculated Raman spectra for the free triplet anion and the considered anion triplet complexes display some resemblance to each other, consistent with the structural similarity for the free triplet anion and H-bonded triplet anion complexes. From the calculations, the stabilization energy is estimated to be ∼14.2 and 12.5 kcal/mol for the H-bond interaction with the oxygen of the carbonyl and hydroxy moiety, respectively (Table 2S in the Supporting Information). These H-bonding energies are stronger than the corresponding energies for the neutral HA triplet H-bonded complexes (6.8 and 4.9 kcal/mol, respectively, see below Table 7S in the Supporting Information). We thus believe that the triplet anion is in the form of an H-bonded

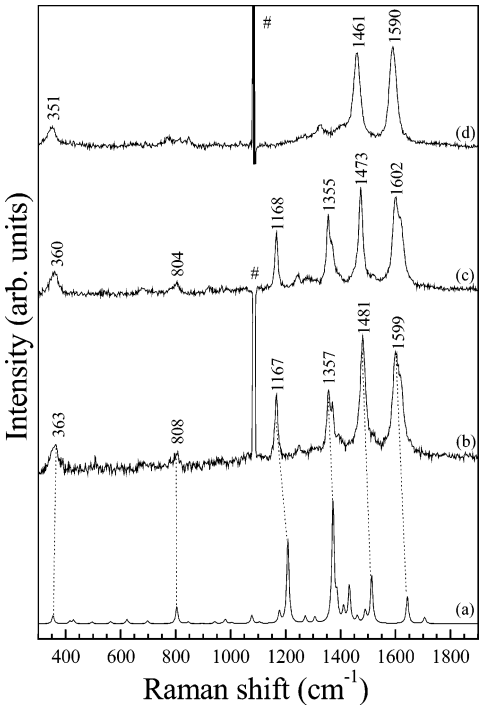

FIGURE 6. Comparison of the experimental ns-TR^3 spectrum (b) of the HA triplet anion obtained at 40 ns displayed in Figure 2b to the UB3LYP/6-311G(d,p) DFT-calculated normal Raman spectrum (a) of the HA anion triplet complex. The # in the experimental spectrum marks a stray laser line. Nanosecond-TR^3 spectra of the HA triplet anion obtained for the isotopically substituted HA-^{13}C (c) and HA-D_4 (d) with 267 nm pump and 416 nm probe wavelengths are also shown to help with the assignment of the experimental spectrum.

complex with a structure similar to that of the ^{3}HA′$^-$−2H_2O displayed in Figure 5.

Figure 6 displays a comparison between the experimental TR^3 spectrum obtained at 40 ns in Figure 2b to the calculated normal Raman spectrum of the ^{3}HA′$^-$−2H_2O triplet anion complex. A Lorentzian function with a 10 cm^{-1} bandwidth was used to generate the calculated Raman spectrum from the vibrational frequencies and relative Raman intensities obtained from the UB3LYP/6-311G(d,p) calculation. The calculated spectra for free ^{3}HA$^-$ and the one water anion triplet H-bonded complexes are presented in Figure 6S in the Supporting Information. Nanosecond TR^3 spectra of isotopically substituted HA-^{13}C and HA-D_4 obtained under the same experimental condition as the spectra shown in Figure 2b are also presented in Figure 6 to help assign the vibrational features. Inspection of Figure 6 reveals that the calculated normal Raman spectrum exhibits reasonable agreement with the experimental TR^3 spectrum for the second species formed from the decay of the HA triplet state. This indicates and confirms the second triplet nature species observed in Figure 2 is due to the triplet anion species and that we directly observe the deprotonation reaction of HA triplet (in the H-bonded form) to generate the HA triplet anion using the TR^3 measurement (Figure 2). The experimental (Figure 6b) and calculated (Figure 6a) spectra for the HA anion triplet show moderate differences in their relative Raman intensity pattern, and this is probably due to the experimental spectrum being resonantly enhanced while the calculated spectrum is a nonresonant Raman one. Preliminary Raman band assignments of the experimental features were made based on the observed isotopic shift in frequencies as well as direct correlation between the experimental and calculated spectra shown in Figure 6. Table 1 lists these tentative vibrational assignments with the nominal descriptions of the normal modes. The isotopic shifts observed in the spectrum from HA-^{13}C (Figure 6c) and HA-D_4 (Figure 6d) and the calculated frequencies for the triplet anion of HA-^{13}C are also given in Table 1. The calculated results for HA-D_4 together with the corresponding vibrational assignments are given separately in Table 3S in the Supporting Information due to obvious differences in the vibrational components for many vibrational modes as well as the different order of the nominal modes.

Most of the Raman bands observed for the TR^3 spectra of the triplet anion are due to vibrations associated with the ring C−C stretching and C−H bending motions. For example, the 1599, 1481, 808, and 363 cm^{-1} bands are predominated by various ring C−C vibrations and the features at 1371 and 1167 cm^{-1} are contributed mainly from the ring C−H in-plane bending motions. These assignments are consistent with the isotopic shift behavior observed in the spectra from HA-^{13}C and HA-D_4 (Figure 6, parts c and d). A vibrational feature showing an obvious isotopic shift upon the carbonyl ^{13}C substitution is the 1481 cm^{-1} band in the HA spectrum (1473 cm^{-1} in the spectrum from HA-^{13}C). This is in agreement with the calculated results showing that the vibration accounting for this band has a substantial contribution from the carbonyl stretching motion. On the other hand, the obvious sensitivity of the normal bands to the ring deuteration confirms their attributions to the ring-related vibrational features. For example, the 1599, 808, and 365 cm^{-1} features in the normal HA spectrum are observed to shift down to 1590, 771, and 351 cm^{-1}, respectively, in the HA-D_4 spectrum. The amount of these shifts are characteristic for the assigned ring C−C stretching vibrations.[15b,20] Further, the absence of the 1167 cm^{-1} bands in the ring-deuterated spectrum coincides with their ring C−H in-plane bending assignment. The ring C−H in-plane bending vibrations have been observed generally to shift down by ∼300 cm^{-1} upon the ring deuteration.[20] According to the calculations, the weak feature at 842 cm^{-1} in the HA-D_4 spectrum could be the counterpart of the 1167 cm^{-1} feature in the normal HA spectrum. The different resonance enhancement pattern between the spectrum from HA-D_4 and those from the normal HA and HA-^{13}C could be due to changes in vibrational coupling pattern and redistribution of potential energy related to the relevant modes induced by the ring deuteration.[15b,20]

C. TR^3 Observation of the Formation of the Deprotonated Ground-State Species and Its Assignment. Nanosecond-TR^3 obtained after 266 nm pho-

(20) (a) Kwok, W. M.; Ma, C.; Matousek, P.; Parker, A. W.; Phillips, D.; Toner, W. T.; Towrie, M.; Umapathy, S. *J. Phys. Chem. A* **2001**, *105*, 984−990. (b) Kwok, W. M.; Ma, C.; Parker, A. W.; Phillips, D.; Towrie, M.; Matousek, P.; Phillips, D. L. *J. Chem. Phys.* **2000**, *113*, 7471−7478. (c) Ma, C.; Kwok, W. M.; Matousek, P.; Parker, A. W.; Phillips, D.; Toner, W. T.; Towrie, M. *J. Photochem. Photobiol., A* **2001**, *142*, 177−185. (d) Kwok, W. M.; Gould, I.; Ma, C.; Puranik, M.; Umapathy, S.; Matousek, P.; Parker, A. W.; Phillips, D.; Toner, W. T.; Towrie, M. *Phys. Chem. Chem. Phys.* **2001**, *3*, 2424−2432.

TABLE 1. Observed and Calculated Vibrational Frequencies (cm^{-1}) and Tentative Assignments for the HA Triplet Anion[a]

exptl			calcd			
			frequency			
$^3HA'^-$	^3HA-$^{13}C'^-$	^3HA-$D_4'^-$		$^3HA'^-$	^3HA-$^{13}C'^-$	description
363	360	351	ν14	354	353	skeleton i.p. deformation
			ν15	360	355	skeleton o.p. deformation
			ν16	400	400	ring C−C o.p. deformation + H4−O4−H5 rocking
			ν17	415	414	H4−O4−H5 rocking + skeleton i.p. deformation
			ν18	426	426	H2−O3−H3 rocking
			ν19	429	428	H4−O4−H5 rocking
			ν20	496	494	skeleton i.p. deformation
			ν21	521	517	C1−O1, C4−C7 o.p. bending + ring C−H o.p. bending
			ν22	564	562	skeleton i.p. deformation
			ν23	623	623	ring C−C i.p. deformation
			ν24	698	696	skeleton i.p. deformation
			ν25	717	716	ring C−C o.p. deformation
			ν26	767	767	ring C−H o.p. bending
808	804	771	ν27	804	804	ring C−C i.p. deformation + O4−H4 bending
			ν28	807	807	ring C−H o.p. bending
			ν29	846	846	O4−H4 bending
			ν30	895	895	O3−H2 bending
			ν31	943	939	CH_3 rocking + ring C−C i.p. deformation
			ν32	967	966	ring C−H o.p. bending
			ν33	976	976	ring C−H o.p. bending
			ν34	981	979	CH_3 rocking + ring C−C i.p. deformation
			ν35	1005	1000	CH_3 deformation
			ν36	1077	1073	CH_3 rocking + ring C−C i.p. deformation
			ν37	1105	1105	ring C−H i.p. bending
			ν38	1178	1177	ring C−H i.p. bending
1167	1168	842	ν39	1209	1209	ring C−C stretching + ring C−H i.p. bending
			ν40	1272	1267	ring C−C stretching + ring C−H i.p. bending
			ν41	1307	1294	ring C−H i.p. bending + C4−C7−C8 stretching
1357	1355	1322	ν42	1373	1369	C1−O1 stretching + ring C−H i.p. bending
			ν43	1387	1387	CH_3 umbrella
			ν44	1411	1399	ring C−H i.p. bending
			ν45	1432	1420	C7−O2, ring C−C stretching + CH_3 deformation
			ν46	1461	1460	ring C−C stretching
			ν47	1488	1488	CH_3 deformation + ring C−H i.p. bending + C1−O1 stretching
			ν48	1491	1491	CH_3 deformation
1481	1473	1461	ν49	1514	1502	C7−O2, C1−O1, ring C−C stretching + CH_3 deformation
1599	1602	1590	ν50	1644	1642	ring C−C, C1−O1 stretching

[a] Note: i.p., in-plane; o.p., out-of-plane.

tolysis of HA in water using a different probe wavelength (341.5 nm) observed the formation and decay of other species, and these TR^3 spectra are shown in Figure 7. The time dependence of the Raman features displayed in Figure 7 indicates that there exist two sets of bands following distinctly different kinetics that can be associated with two different transient species. The species having noticeable Raman bands at 705, 843, 1074, 1527, 1567, and 1617 cm^{-1} (features in red as displayed in Figure 7) appears and approaches a maximum intensity at about 120 ns and then decays over the next 600 ns. The 705 cm^{-1} Raman band integrated area was used to follow the dynamics of this transient species, and this kinetics is displayed in Figure 3 along with the decay kinetics of the HA triplet anion described above. The kinetics of this new species can be fit well by a two-exponential function composed of a growth component with a time constant of about 90 ns and a decay component with a time constant of about 200 ns.

Our results for the 341.5 nm probe TR^3 experiments are consistent with previous transient absorption studies of Givens, Wirz, and co-workers.[4a] This study shows that ultraviolet photolysis of HA in neutral water solution produced an intermediate with $\lambda_{max} = 325$ nm absorption band (our 341.5 nm probe wavelength for the TR^3 spectra displayed in Figure 7 is resonant with this absorption) whose yield and lifetime are not affected by oxygen and the absorption spectrum is identical to that of the HA ground-state anion in aqueous base. This suggests that the new intermediate we observed in the TR^3 experiments using the 341.5 nm probe wavelength is the anion ground-state species. To confirm this assignment, we obtained a resonance Raman spectrum of the HA anion using a 341.5 nm excitation wavelength in water/NaOH (0.1 M) basic solution. Figure 8 shows a comparison of this spectrum to that of the 100 ns transient TR^3 spectrum of this particular new transient recorded with the 341.5 nm probe wavelength in neutral water solution shown in Figure 7. Comparison of the spectra reveals they are essentially identical to each other, and this confirms that the intermediate of interest is indeed the HA ground-state anion.

With the definitive attribution of the new species to the HA ground-state anion, comparison of the anion ground-state kinetics with that for the anion triplet state observed for the same sample and an analogous experiment probed with a 416 nm wavelength (Figure 3) reveals that the growth of the anion ground state observed with the 341.5 nm probe wavelength correlates well with the decay of the anion triplet state observed with the 416

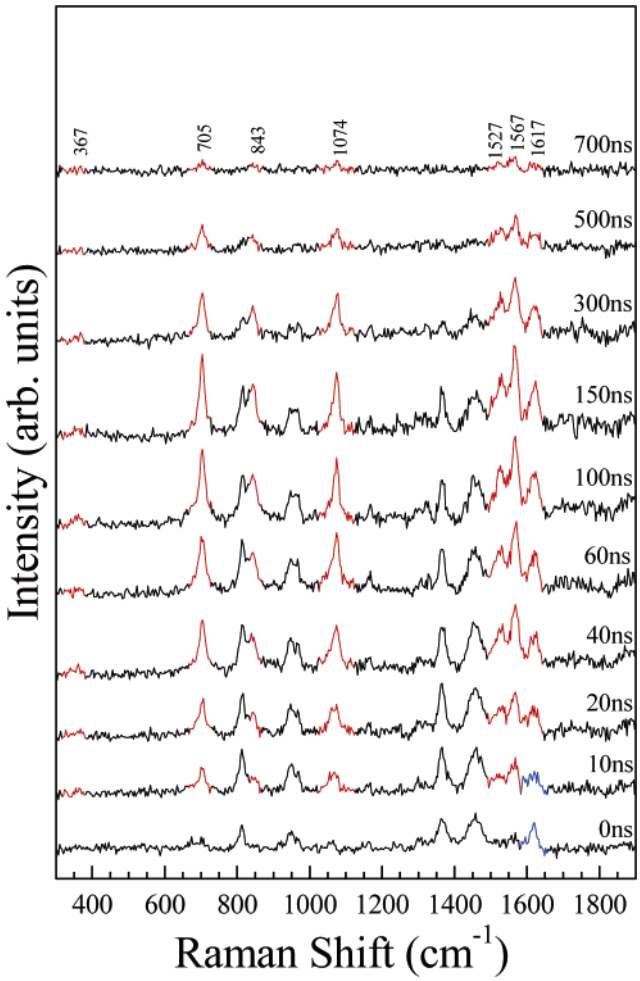

FIGURE 7. Nanosecond-TR^3 spectra of HA in water solution obtained at various time delays with 267 nm pump and 341.5 nm probe wavelengths. Features in blue are due to the neutral HA triplet state. See the text for details of the attributions of other features.

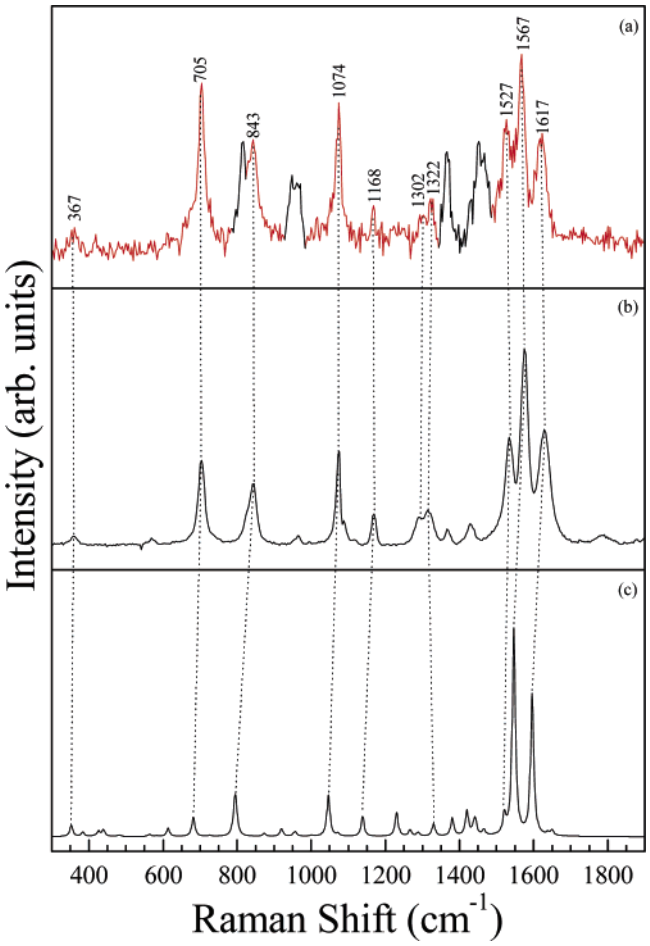

FIGURE 8. Comparison of the ns-TR^3 spectrum (a) obtained at a 100 ns time delay in Figure 7 to the 341.5 nm resonance Raman spectrum of the ground-state HA anion (b) obtained in water/NaOH (0.1 M) solution. B3LYP/6-311G(d,p) DFT-calculated normal Raman spectrum of the HA anion ground state (c) is also shown to compare and help with the assignment of the experimental spectra. Features in back shown in spectrum (a) are due the unidentified species "X" (see the text for details).

nm probe wavelength. This indicates that the anion ground state is produced directly from the anion triplet state and the estimated 90 ns time constant corresponds to time of the ISC conversion for deactivation of the anion triplet state to the anion ground state.

The structure of the anion ground state and the effect of the H-bond interactions were determined from the B3LYP/6-311G(d,p) calculations. Analogous to the DFT calculations for the H-bonded complex of the HA anion triplet, the H-bonded ground-state calculation was done also by considering the solvent water molecules H-bonded with oxygen lone pairs of the carbonyl and deprotonated hydroxy moieties. Similar to the calculated results for the anion triplet complexes, a planar structure was found for the anion ground state. The H-bonding conformations in the ground state were close to that for the corresponding triplet state with the H-bonding resulting in small and localized modification of the anion structure in the ground state. The calculated structural parameters for the free HA anion ground state (denoted as HA^- hereafter) and the anion complex containing two H-bonded water molecules (denoted as $HA'^- - 2H_2O$ hereafter) along with the total energies and the H-bond stabilization energy are listed in Table 4S. The corresponding results for the ground-state complexes involving one water are given in Table 5S of the Supporting Information. It can be seen from the tables that the stabilization energies are 12.1 and 15.1 kcal/mol, respectively, for the H-bonding at the carbonyl and deprotonated hydroxy site (Table 5S in the Supporting Information). Comparison with the corresponding triplet state data indicates that the strength of the H-bond interaction is slightly weakened for the carbonyl site, whereas it is strengthened for the deprotonated hydroxy oxygen. It is thus reasonable to believe that the HA anion ground state also exists in the form of an H-bonded complex. Along with the structural resemblance, the calculation results in similar Raman spectra for the free and H-bonded anion ground states. Comparison of the calculated spectrum for the $HA'^- - 2H_2O$ with the experimental resonance Raman spectra obtained for the ground-state HA anion is displayed in Figure 8. The reasonable agreement between the calculated and experimental spectra allows straightforward assignments of the vibrational features observed in the experimental spectra. Table 2 lists the experimen-

TABLE 2. Observed and Calculated Vibrational Frequencies (cm^{-1}) and Tentative Assignments for the HA Ground-State Anion[a]

exptl	calcd		
	frequency		description
367	ν14	352	skeleton i.p. deformation
	ν15	383	H2−O3−H3 rocking
	ν16	415	ring C−C o.p. deformation
	ν17	426	H4−O4−H5 rocking
	ν18	439	H4−O4−H5 rocking + skeleton i.p. deformation
	ν19	479	ring C−H o.p. bending
	ν20	484	C1−O1 i.p. bending + C4−C7−C8 i.p. bending
	ν21	563	ring C−C i.p. deformation + C7−O2 i.p. bending
	ν22	583	C4−C7 o.p. bending + CH_3 rocking + ring C−H o.p. bending
	ν23	613	ring C−C i.p. deformation
705	ν24	682	skeleton i.p. deformation
	ν25	727	ring C−C o.p. deformation + ring C−H o.p. bending
	ν26	789	ring C−H o.p. bending
843	ν27	795	ring C−C i.p. deformation
	ν28	800	O3−H2 bending
	ν29	839	ring C−H o.p. bending + C1−O1 o.p. bending
	ν30	873	O4−H4 bending
	ν31	920	CH_3 rocking
	ν32	950	ring C−H o.p. bending
	ν33	956	ring C−H o.p. bending
	ν34	957	ring C−H o.p. bending
	ν35	1000	CH_3 deformation + C4−C7 o.p. bending
1074	ν36	1046	CH_3 rocking + ring C−C i.p. deformation
	ν37	1072	ring C−H i.p. bending
1168	ν38	1139	ring C−H i.p. bending
	ν39	1230	ring C−C stretching + ring C−H i.p. bending
	ν40	1267	ring C−C stretching + ring C−H i.p. bending
	ν41	1288	ring C−H i.p. bending + C4−C7−C8 stretching
1322	ν42	1330	CH_3 umbrella + ring C−H i.p. bending
	ν43	1380	C1−O1, C4−C7 stretching + ring C−H i.p. bending
	ν44	1420	CH_3 deformation
	ν45	1437	ring C−C stretching + CH_3 deformation
	ν46	1442	CH_3 deformation
	ν47	1466	ring C−C stretching
1527	ν48	1521	ring C−C, C1−O1 stretching
1567	ν49	1547	ring C−C stretching
1617	ν50	1596	ring C−C, C1−O1 stretching
	ν51	1638	H2−O3−H3 bending
	ν52	1650	H4−O4−H5 bending

[a] Note: i.p., in-plane; o.p., out-of-plane.

tal and calculated frequencies and the corresponding vibrational attribution of these features.

Inspection of Figure 7 shows that, besides the series of Raman bands from the HA ground-state anion species, the residual strong features at ~810, 945, 965, 1370, and 1455 cm^{-1} (features in black as displayed in Figure 7) are obviously from another alternative intermediate. The temporal evolution of this series of bands reveals a single-exponential decay kinetics with a lifetime of ~88 ± 7 ns. The formation and decay times of this species appear to be similar to that of the HA anion triplet state detected in the ns-TR^3 spectra using the 416 ns probe wavelength (Figure 2b and Figure 3). Although there is closeness in the kinetic behavior, the probable attribution of these vibrational features to the anion triplet state can be ruled out by the results from our TR^3 experiments done for HA in buffered acid water solution using the 267 nm pump and 341.5 or 416 nm probe wavelengths. These experiments reveal a total absence of the Raman features from the anion species (both the triplet and ground state), whereas the exclusive appearance of the above-mentioned features observed in the 341.5 nm probe spectra (features in black as shown in Figure 7) and the intermediate was found to stem directly form the HA triplet state. A representative result of ns-TR^3 spectra obtained for HA in pH = 1 buffered water solution with the 341.5 nm probe wavelength is presented in Figure 7S in the Supporting Information. The spectra show clearly the sole observation of this transient species in the acidic environment, in contrast to the situation in the neutral water condition where both the HA ground-state anion and this intermediate have been detected (see spectra shown in Figure 7). This indicates that formation of the latter species is favored strongly by the existence of excess protons in the water solution. We note that the TA work by Givens, Wirz, and co-workers reports a protonated species at low pH value showing an absorption band with a maxima around 350 nm.[4a] Since the 341.5 nm probe wavelength is resonant with this absorption, we believe that the corresponding Raman features (~810, 945, 965, 1370, and 1455 cm^{-1}) we observed in Figure 7 are from the same species as that observed in the TA study. Probable attribution of this intermediate includes the quinonoid enol triplet of HA[4a,6a] and the cationic species (most possibly in its triplet) generated by protonation of the carbonyl oxygen of the neutral HA triplet.[6a] Both of the attributions are associated with the increased basicity and acidity of the carbonyl oxygen and

phenolic hydrogen, respectively, in the triplet relative to that of the ground state. However, a preliminary comparison of the DFT-calculated Raman spectra with the experimentally obtained spectrum reveals that neither of these two species appears to provide a reasonable match to the experimental data. Providing the generally good reproduction of the DFT-calculated spectrum to the experimental spectra for the HA and *p*-HP related compounds, this may imply that an alternative assignment to the observed transient species is needed. Further experimental and theoretical work is planned to explore the explicit identification of this species, and we temporally denoted it as "X" hereafter in this paper.

D. Structures and Properties of the HA Triplet, HA Anion Triplet, and Anion Ground State in Water Solution. From the preceding sections, it is clear that for the HA anion species, both the triplet and ground state have planar structures (C_s symmetry) with the hydroxy and carbonyl moieties lying in the plane defined by the phenyl ring. They also both exist in the form of H-bonded complexes with two solvent water molecules H-bonded, respectively, to the oxygen atom of the carbonyl and deprotonated hydroxy moieties. Our DFT calculations reveal that the geometries of the H-bonded complexes of these anion species are generally very close to those of their corresponding free counterparts.

This is significantly different from the case of the neutral HA triplet state. Our previous combined TR[3] and DFT study on HA in neat acetonitrile indicates that the free HA triplet ^{3}HA ($^3\pi\pi^*$ nature) is nonplanar (C_1 symmetry) with the $-C(O)CH_3$ group being twisted out of the molecular plane by about 16° and the CH_3 group rotated around the C(O)−C bond by about 37°.[15b] This deviation of the aromatic carbonyl $\pi\pi^*$ triplet from planar structure has long been associated with the strong vibrational coupling between the $\pi\pi^*$ triplet and the next nearby $n\pi^*$ triplet.[21,22] However, UB3LYP/6-311G(d,p) DFT calculations on the H-bonded complex of the neutral HA triplet (^{3}HA′) containing up to three water molecules H-bonded, respectively, with the hydroxy hydrogen and oxygen lone pairs of the carbonyl and hydroxy moieties results in a planar structure and substantially increased quinoidal character of the phenyl ring compared to that of the free ^{3}HA. The optimized structure of the ^{3}HA′-3H_2O complex is displayed in Figure 9, and the structures of the ^{3}HA′ complexes involving one water molecule are presented in Figure 8S of the Supporting Information. The DFT calculations were also done for the corresponding ground-state HA−water complexes, and similar H-bond topologies were found comparable to those of the HA triplet complex.

Like the cases of the HA anion triplet and the ground state, the H-bond interactions lead to only small and localized structural modification to the HA ground state. However, the H-bond interactions result in significant perturbation to the HA triplet state. Table 6S lists the calculated geometric parameters and energy result for the free ^{3}HA and the ^{3}HA′−3H_2O. The corresponding data for the HA triplet complexes containing one water molecule and those for the HA ground-state H-bonded complexes are presented in Tables 7S and 8S, respectively, in the Supporting Information. The H-bond topologies in the neutral triplet complexes are similar to those of their ground-state counterparts. The H-bond strengths of the carbonyl oxygen (6.8 kcal/mol), hydroxyl oxygen (4.9 kcal/mol), and hydroxyl hydrogen (9.9 kcal/mol) located triplet complexes are somewhat stronger than that of the ground-state counterparts (6.7, 4.5, and 9.2 kcal/mol, respectively, Tables 7S and 8S in the Supporting Information). The increased strength of the H-bond at the carbonyl oxygen (as an H-bond acceptor) and the hydroxy hydrogen (as an H-bond donor) is in agreement with the general expectation that the carbonyl oxygen of the aromatic carbonyl compound becomes more basic in the $\pi\pi^*$ triplet than in their ground state and the hydroxyl hydrogen becomes more acidic in the excited state than in the ground state.

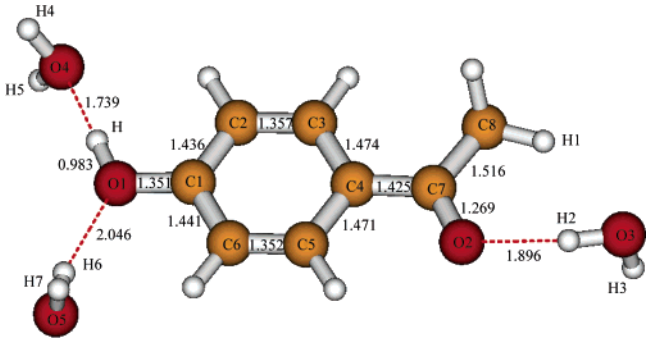

FIGURE 9. Optimized geometry of the H-bonded HA triplet complex containing three water molecules obtained from the DFT calculations using the UB3LYP method with a 6-311G-(d,p) basis set. Bond lengths (in Å) are labeled for the C−C, C−O, and H-bond associated bonds.

According to the values of the H-bond stabilization energy (Table 7S in the Supporting Information), the carbonyl oxygen and hydroxy hydrogen located triplet complexes are more stable than the hydroxy oxygen located complex. This comparison of the H-bond strengths is consistent with the extent of structural modification caused by the respective H-bond interactions. The calculated structural data (Table 7S) indicate that the carbonyl oxygen and hydroxy hydrogen located H-bonds lead to a similar quinoidal planar structure (also similar to the geometry of the ^{3}HA′-3H_2O complex displayed in Figure 9 and Table 6S) that is substantially different from that of the ^{3}HA free triplet. However, the hydroxy oxygen sited H-bond causes only a small modification, and the corresponding complex has a twisted structure similar to that of the ^{3}HA free triplet. Consistently, the calculated Raman spectra for the H-bonded triplets containing the carbonyl oxygen and hydroxy hydrogen located H-bonds display substantial differences from that of the free HA triplet. In contrast, the spectrum of the complex involving only the hydroxy oxygen H-bond is close to the free triplet spectrum. This implies the importance of the carbonyl and hydroxy hydrogen sited H-bond interactions in accounting for the structural modifications associated with the H-bonding effect, and therefore they are mainly responsible for the spectral difference observed experimentally in the solution of water in relationship to that in acetonitrile. This is

(21) Kiritani, M.; Yoshii, T.; Hirota, N. *J. Phys. Chem.* **1994**, *98*, 11265−11268.
(22) (a) Lim, E. C.; Li, Y. H.; Li, R. *J. Chem. Phys.* **1970**, *53*, 2443−2448. (b) Li, R.; Lim, E. C. *J. Chem. Phys.* **1972**, *57*, 605−612. (c) Li, Y. H.; Lim, E. C. *Chem. Phys. Lett.* **1970**, *7*, 15−18.

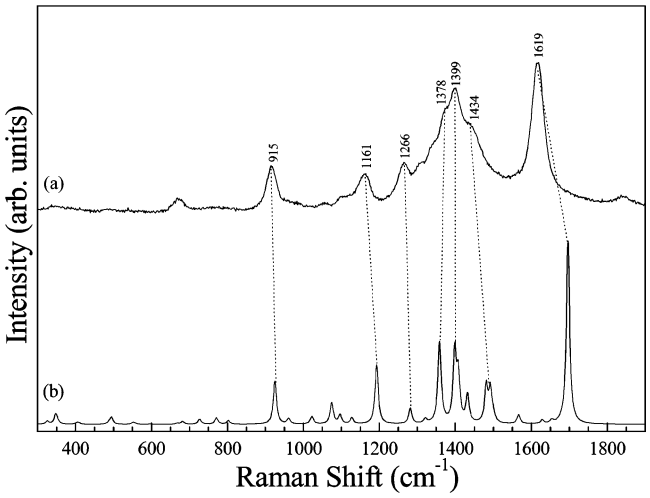

FIGURE 10. Comparison of the ps-TR[3] spectrum (a) obtained at a 50 ps time delay in Figure 2a to the UB3LYP/6-311G-(d,p) DFT-calculated normal Raman spectrum of the HA H-bonded triplet complex containing three water molecules.

confirmed indeed by reasonably good agreement between the calculated Raman spectrum of the ^{3}HA′-3H_2O complex to the HA triplet TR[3] spectrum recorded in water solution (the 50 ps spectrum in Figure 2).

A comparison between the experimental and calculated spectrum for the HA triplet in water solution is shown in Figure 10. The corresponding frequency and related vibrational assignments are given in Table 3. The calculated normal Raman spectra for the triplet complexes involving one H-bonded water molecule are displayed in Figure 9S of the Supporting Information. One characteristic change in the TR[3] spectra is the frequency upshift (by ~25 cm^{-1}) of the ring center C−C stretching vibration on going from the spectrum in acetonitrile (at ~1594 cm^{-1})[15b] to that in water solution (at 1619 cm^{-1}). This manifests the increased quinoidal ring conformation in the H-bonded triplet complex compared to that in the free triplet. From the calculated structural data (Table 6S) it can be seen that the H-bonded carbonyl C−O bond length is shorter (by ~0.05 Å) in the H-bonded triplet complex than in the free triplet. This is significant since the H-bond leads generally to an increase of the bond length for the H-bonded acceptor group,[23−28] like that for the H-bonded complexes of the HA ground state and anion species (see Table 8S in the Supporting Information). The specific difference in the carbonyl bond length between the H-bonded and free HA triplet is an indication of the different electronic property for these two kinds of triplet states. The free HA has a delocalized $\pi\pi^*$ triplet with the π^* electron populated on both the ring and carbonyl moieties;[15b] while the H-bonded HA complexes have a ring-localized biradical $\pi\pi^*$ triplet. The substantial differences in the structural and electronic properties imply that the H-bonded HA triplet complexes can be considered as a distinct triplet species from that of the free HA triplet. This is closely analogous to the H-bond effect we discussed previously for the triplet state of MAP.[17] The resemblance between the HA and MAP in terms of the intrinsic properties of their triplets[15b,17] and relevant H-bonding effect on the triplets[17] is within the expectation that there is a similar electronic effect of the para-substituted group hydroxy and methoxy to the phenacyl chromophore. It has been demonstrated that, for the MAP triplet, the H-bonding interaction can lead to not only a geometric change but also a pronounced longer triplet lifetime than that of the free triplet.[17] In comparison to to MAP, the additional functionality of the hydroxy group to be able to ionize/deprotonate in the HA accounts for the much shorter triplet lifetime in water (~10 ns) than in acetonitrile (40 ns)[15b] solution, and the HA triplet deprotonation reaction is actually associated with the hydroxy hydrogen located intermolecular H-bonding interaction. Furthermore, the importance of the H-bonding interaction on the anions of the HA triplet and ground state is reflected by the larger H-bonding stabilization energies calculated for these anions than those of the respective neutral counterparts.

Considering the small influence of the leaving group on the triplet property of the *p*-HP cage,[15a,b] the H-bonded effect on the triplet structure discussed here for HP and that before for MAP is expected to apply also to the *p*-HP phototrigger compounds. It is thus believed that the triplet precursor for the photodeprotection reaction of the *p*-HP phototrigger compound is the H-bonded triplet complex with a planar and ring-localized biradical structure. In this respect, the solvent water influence on assisting the heterolysis cleavage and the nucleofuge nature of the leaving group could play a crucial role in driving the deprotection reaction for *p*-HP phototrigger compounds.

The HA triplet state deprotonation (or ionization reaction) is intrinsically a direct result of the particular H-bonding interaction with the HA hydroxy moiety as a proton donor and the solvent water molecule as the proton acceptor. As illustrated in the preceding paragraph, the increased acidity of the hydroxy moiety in the triplet compared to that in the ground state (pK_a of ground-state and triplet HA is ~7.9 and 3.6, respectively[4a]) leads to the strengthening of this H-bond interaction upon excitation to the triplet manifold (substantiated by the increased H-bond stabilization energy as mentioned above), and this could consequently result in the transfer of the HA hydroxyl proton to the solvent water molecule, that is, occurrence of the deprotonation/ionization reaction. The facilitation of the triplet H-bonding effect to the deprotonation reaction is consistent with the fact that the deprotonation reaction does not occur in neat acetonitrile solvent where the intermolecular solute−solvent H-bonding interaction is absent. It is also reflected by the similarity in the structure for the H-bonded complex of the anion triplet to that of the neutral triplet. From Tables 1S and 6S, one can find that the structural parameters in terms of the phenyl ring and the C(O)-CH_3 moieties are not much different for the H-bonded complexes of the HA anion triplet (^{3}HA′−2H_2O) and the

(23) Kwok, W. M.; George, M. W.; Grills, D. C.; Ma, C.; Matousek, P.; Parker, A. W.; Phillips, D.; Toner, W. T.; Towrie, M. *Angew. Chem., Int. Ed.* **2003**, *42*, 1826−1830.
(24) Scaiano, J. C. *J. Am. Chem. Soc.* **1980**, *102*, 7747−7753.
(25) Kagiya, T.; Sumida, Y.; Inoue, T. *Bull. Chem. Soc. Jpn.* **1968**, *41*, 767−773.
(26) Allerhand, A.; Schleyer, P. v. R. *J. Am. Chem. Soc.* **1963**, *85*, 371−380.
(27) Fuson, N.; Josien, M.; Shelton, E. M. *J. Am. Chem. Soc.* **1954**, *76*, 2526−2533.
(28) Woutersen, S.; Mu, Y.; Stock, G.; Hamm, P. *Chem. Phys.* **2001**, *266*, 137−147.

TABLE 3. Observed and Calculated Vibrational Frequencies (cm^{-1}) and Tentative Assignments for the HA Triplet State (in the Form of the H-Bonded Complex)[a]

exptl	calcd		
	frequency		description
	ν21	326	skeleton o.p. deformation + H2−O3−H4 rocking
	ν22	348	skeleton i.p.deformation + O5−H6 i.p.bending
	ν23	354	H2−O3−H4 rocking + ring C−C o.p. deformation
	ν24	404	ring C−C o.p. deformation
	ν25	410	skeleton i.p.deformation + O5−H6 i.p. bending
	ν26	487	skeleton i.p. deformation + O5−H6 i.p. bending
	ν27	495	ring C−C o.p. deformation + C4−C7 o.p. deformation
	ν28	552	O5−H6 i.p. bending + skeleton i.p. deformation
	ν29	559	O5−H6 i.p. bending
	ν30	596	ring i.p. deformation
	ν31	668	ring o.p. deformation
675	ν32	682	skeleton i.p. deformation
	ν33	726	O3−H2 i.p. bending
	ν34	730	ring C−H o.p. deformation
	ν35	771	ring C−C i.p. deformation
	ν36	802	ring C−H + O1−H o.p. bending + ring C−C o.p. bending
	ν37	881	O1−H o.p. bending
915	ν38	925	ring C−C stretching + CH_3 rocking
	ν39	961	CH_3 rocking + ring C−C stretching
	ν40	963	ring C−H o.p. deformation + O1−H o.p. deformation
	ν41	1020	ring C−H o.p. bending + CH_3 deformation
	ν42	1023	CH_3 deformation + ring C−H i.p. bending
	ν43	1075	CH_3 rocking + ring C−C stretching
	ν44	1097	ring C−C stretching
	ν45	1128	ring C−H i.p. bending + O1−H i.p. bending + ring C−C stretching
1161	ν46	1193	ring C−H i.p. bending
1266	ν47	1281	ring C−C stretching + ring C−H, O1−H i.p. bending
b	ν48	1321	ring C−H i.p. bending + C1−O1 stretching
1378	ν49	1358	C4−C7−O2 stretching + ring C−H i.p. bending
b	ν50	1365	ring C−H i.p. bending + C4−C7−C8 stretching + O1−H i.p. bending
1399	ν51	1399	CH_3 umbrella + C7−O2 stretching + ring C−H, O1−H i.p. bending
b	ν52	1408	CH_3 umbrella + ring C−C, C7−O2 stretching + O1−H i.p. bending
b	ν53	1432	O1−H i.p. bending
1434	ν54	1482	ring C−C + C1−O1 stretching + CH_3 umbrella
	ν55	1492	CH_3 deformation + ring C−H i.p. bending
	ν56	1500	CH_3 deformation
	ν57	1567	ring C−C stretching + O1−H1 i.p. bending
	ν58	1629	H4−O4−H5 bending
	ν59	1654	H6−O5−H7 bending
	ν60	1680	H2−O3−H3 bending
1619	ν61	1697	ring C−C stretching + C1−O1 stretching

[a] Note: i.p., in-plane; o.p., out-of-plane. [b] Broad and overlapped bands.

neutral triplet (^{3}HA−3H_2O) although the C−O bond connecting the ring and hydroxy group is shortened by ∼0.05 Å in the anion triplet than in the neutral triplet. This structural resemblance in the ring and carbonyl chromophore for the anion and neutral triplet state may provide an explanation for the similar absorption bands reported for the two species in the TA study by Givens, Wirz, and co-workers.[4a]

Compared with the H-bonded complex of the HA ground state (HA′−3H_2O, Table 8S in the Supporting Information), the H-bonded complex of the HA ground-state anion (HA′ anion-2H_2O in Table 4S) has an increased quinoidal ring and a substantial shortening of the C−O (by ∼0.09 Å) and C−C (by ∼0.04 Å) bonding connecting the ring and hydroxyl and carbonyl groups, respectively. This reflects the increased conjugation of the hydroxy oxygen lone pair to the ring and carbonyl π systems in the ground-state anion compared to that in the neutral HA. This extra conjugation leads to a larger degree of conjugation in the system for the anion species compared to that of the neutral one. This may account for the red shift of the absorption band (peaking at ∼320 nm) for the anion species relative to that for the neutral compound (peaking at ∼270 nm, see Figure 1).

E. Dynamics of the HA Triplet Deprotonation and Its Implication for the *p*-HP Photorelease Reaction. Our combined TR^3 results obtained with ∼400 nm (Figure 2) and ∼341.5 nm (Figure 7) probe wavelengths after ultraviolet photolysis of HA in neutral water solutions indicate that the HA triplet is formed within several picoseconds (with ∼2 ps time constant) by ISC from the S_1 excited state and subsequently decays on the nanosecond time scale (with a ∼10 ns time constant) resulting in the simultaneous generation of the HA triplet anion by the deprotonation reaction and an unidentified X species by an unknown protonation-related process. The triplet anion and X species then decay with time constants of about 95 ns (Figure 3) and 88 ns, respectively. The decay of the triplet anion species leads to formation of the anion ground-state intermediate that was found to have a lifetime of ∼200 ns (Figure 3). Provided the ground-state HA has a pK_a of 7.9,[4a] it is believed that, in the neutral water solution, the newly generated HA anion ground-state molecules are further

protonated by the solvent water molecules and consequently return back to the HA neutral species. As discussed above, all the relevant species exist in the form of the H-bonded complexes, and the hydroxy hydrogen located H-bond interaction facilitates the triplet deprotonation reaction. As to the fate of the X species, it is believed tentatively that it decays back to the ground state of the neutral HA since UV absorption measurements of the HA water solution immediately after the TR^3 measurement indicates no appreciable degradation. Taking together all these dynamics results suggests the following deactivation scheme for ultraviolet photolysis of HA in neutral water solution (the apostrophe labels in the scheme indicate that the species are in the form of H-bonded complexes).

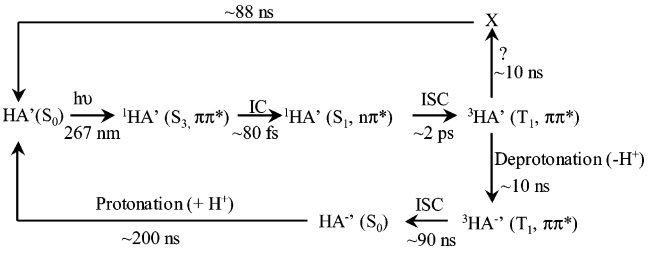

We note that the triplet deactivation channels suggested in the scheme are only in partial agreement with the interpretation presented in previous TA work by Givens, Wirz, and co-workers.[4a] The common aspect between the above scheme and the TA study is the triplet deprotonation pathway leading to generation of the HA triplet anion and the subsequent deactivation of the triplet anion to the ground-state anion; the divergence between the two is on the dynamic order and probably the identification (see above in section C) of the X species denoted here. The TA work proposed that the X species is a reprotonated product generated from HA triplet anion in acid solution and was attributed to the triplet enol of HA. However, our TR^3 result reveals that the dynamics of the formation of the HA anion triplet and X species are parallel competing channels, rather than sequential steps, to account for depopulation of the HA neutral triplet. This conclusion is corroborated by the observation that, in acid solution, direct decay of the HA triplet to the X species becomes significantly faster and consequently blocks the deprotonation-related pathway such that generation of the X species becomes the almost exclusive deactivation pathway of the ^{3}HA triplet.

It is interesting to note that the HA triplet deactivation leading to the deprotonation and parallel formation of the X species in neutral water solution is relatively slow (~10 ns) when compared to the decay of the corresponding triplets of the *p*-hydroxyphenacyl acetate (HPA) and *p*-hydroxyphenacyl diphosphate (HPDP) that have time constants of ~2130 and ~420 ps, respectively, in 50% acetonitrile/50% H_2O solution.[14] The rate of HA triplet deprotonation and related deactivation processes was found to be proportional to the water concentration and is therefore slower in the 50% MeCN/50% H_2O mixed solvent than in neat water solution.[4a] This, along with the expectation that the triplets of HPA and HPDP have similar reaction times as the HA triplet in terms of the triplet deprotonation reaction, implies that some other competing reaction, most probably related to the deprotection reaction, is responsible for the leaving group dependent decay of the triplets of HPA and HPDP in water-containing solvents.

Our TR^3 result here on the HA model compound combined with our previous result on HPA and HPDP provides no evidence for the deprotonation process being involved in the leaving group deprotection process. The results here shown in Figure 2 demonstrates that the HA triplet anion can be detected selectively with the ~400 nm probe wavelength. However, with the same probe wavelengths for the TR^3 measurements on the HPA and HPDP phototrigger compounds, our previous work[14] reveals that vibrational features from the triplet anion intermediate have not been observed at all and only features belonging to the neutral triplets that display single-exponential decay kinetics have been seen in the 50% MeCN/50% H_2O solvent for the two phototrigger compounds. The results for HPDP are also corroborated with the transient absorption study on HPDP in the 50% MeCN/50% H_2O solvent showing the exclusive observation of a single-exponential decay of the HPDP triplet absorption with λ_{max} at ~400 nm.[4a] However, an extra transient absorption band peaking at ~330 nm with nano- to microsecond lifetime, probably due to the anion ground state and the X species, has been reported for photolysis of HPA in 50% MeCN/50% H_2O solvent.[6a] Provided the much better leaving ability of the phosphate leaving group than that of the acetate leaving group (as scaled by pK_a to gauge the stability of the leaving group anion)[29] combined with the slower triplet decay rate for the HPA than HPDP,[14] the additional complexity in the time-resolved observations for HPA in relationship to HPDP indicates that extra competing deactivation channel(s) become(s) operative to depopulate the HPA triplet compared to HPDP. This implies further a strong dependence of the triplet deactivation pathway and probably the deprotection mechanism on the kind of leaving group for the *p*-HP phototrigger compounds. Further work is needed to fully connect the decay of the triplets of phototrigger compounds such as HPA and HPDP in water solutions to the cleavage step and formation of the rearrangement product and leaving group. Direct observation of when the rearrangement product first appears would be helpful to better understand when the cleavage step occurs and which species is undergoing the cleavage. Since the *p*-HP photorelease reaction occurs exclusively in a water-containing environment, it is quite certain from the H-bonding effect discussed in this work that the precursor triplet species to the leaving group deprotection reaction is the H-bonded triplet complex with a planar structure rather than the twisted free triplet as identified previously for these compounds in acetontrile solvent.

Conclusion

We have presented the first time-resolved vibrational spectroscopic observation of the excited-state deprotonation reaction of HA and characterization of its anion products using TR^3 spectroscopy. These spectra combined with DFT calculations were used to characterize the

(29) Schade, B.; Hagen, V.; Schmidt, R.; Herbrich, R.; Krause, E.; Eckardt, T.; Bendig, J. *J. Org. Chem.* **1999**, *64*, 9109−9117.

structure and dynamics of the deprotonation reaction to form HA anions in neutral water solution. DFT calculations based on a hydrogen-bonded complex model containing up to three water molecules were employed to explore the H-bond interactions and their influence on the deprotonation reaction and structures of the intermediates involved in the reaction. The TR^3 spectra (using 400 and 416 nm probe wavelengths) along with the DFT calculations indicate that the HA deprotonation reaction occurs on the triplet manifold with a planar H-bonded HA triplet complex as precursor species. The neutral HA triplet species is formed within several picoseconds and then decays on the nanosecond time scale to produce an HA triplet anion species after the 267 nm photolysis of HA in water solution. The triplet anion species was observed to decay with a time constant of ~90 ns to another species that was probed by additional TR^3 experiments using a 341.5 nm probe wavelength. This species was identified to be the ground-state HA anion species based on the 341.5 nm transient resonance Raman spectrum being essentially identical to the 341.5 nm resonance Raman spectrum of an authentic ground-state anion obtained in a basic NaOH/water solution. The 90 ns time constant thus corresponds to the ISC conversion time from the HA anion triplet to anion ground-state species. The lifetime of the ground-state HA anion was found to be ~200 ns corresponding to the time constant for reprotonation of this species back to neutral HA providing consistent with a pK_a of 7.9 for the HA ground state in water solution. The DFT calculations on the H-bonded complexes of anion triplet and ground-state species suggest that the anion species are in the forms of H-bonded complexes with planar qunioidal structures containing two water molecules H-bonded, respectively, with oxygen lone pairs of the carbonyl and deprotonated hydroxy moieties. The 341.5 nm probe wavelength TR^3 measurement reveals the observation of an additional species that originates directly from the HA neutral triplet and whose formation is favored strongly by the existence of excess of protons in the solvent environment. Further work is required for its identification. A reaction scheme consistent with the preceding experimental results for the photochemistry of HA after ultraviolet photolysis in neutral water solutions was presented. We briefly discuss the possible implications of the model HA photochemistry in water solutions for the photodeprotection reaction of related *p*-HP phototrigger compounds in water solutions.

Acknowledgment. We thank the Research Grants Council of Hong Kong (HKU 7108/02P) and (HKU 1/01C) to D.L.P. for support of this research. W.M.K. thanks the University of Hong Kong for the award of a research assistant Professorship.

Supporting Information Available: Ps- and ns-TR^3 spectra of HA in water obtained at various pump−probe time delays; comparison of the experimental C=O stretching Raman band recorded in water and acetonitrile solvent; decay kinetics for the triplet anion observed in ns-TR^3 spectra of HA in neutral water solution under nitrogen purge condition; kinetics for ground-state bleach recovery revealed by transient absorption measurements of the HA anion in 0.1 M NaOH/water solution after 267 nm photoexcitation; DFT-optimized geometry of HA triplet and triplet anion H-bonded with one water molecule; DFT-calculated normal Raman spectra of free HA triplet and triplet anion and their corresponding complexes containing one H-bonded water molecule; ns-TR^3 spectra of HA (267/342 nm pump−probe) in 0.1 M NaOH/water solution; tabulated DFT-calculated results for structural and energy data (including H-bond stabilization energy for the H-bonded complexes) for various free HA species and H-bonded complexes; observed and calculated vibrational frequencies (cm^{-1}) and tentative assignments for the HA-D_4 triplet anion; Cartesian coordinates for DFT-optimized structures of anion species for HA triplet and ground states. This material is available free of charge via the Internet at http://pubs.acs.org.

JO050761Q